Applying the Optical Theorem in a Finite-Difference Time-Domain Simulation of Light Scattering

Cheng-Hao Tsai, Shih-Hui Chang, and Snow H. Tseng

***Abstract*—The total scattering cross-section (TSCS) is a useful parameter in analyzing light scattering properties. Here we derive a pragmatic relationship of the optical theorem to be employed in a Finite-difference time-domain (FDTD) simulation of light scattering problems. Specifically, the accuracy of the proposed TSCS calculation method is analyzed and compared with other methods.**

***Index Terms*—Electromagnetic scattering by random media, optics, simulation.**

I. Introduction

Utilizing optical wavelengths for sensing purposes such as noninvasive medical diagnostic techniques have attracted much research attention. Regardless of the specific sensing mechanism involved, the fundamental problem is gauging the optical characteristics of a random medium (e.g., biological tissue) by scattered light. This phenomenon can be analyzed using rigorous simulation techniques based upon Maxwell's equations [1]. Commonly employed rigorous simulation techniques include the finite-difference time-domain (FDTD) method [1] and the Pseudospectral time-domain (PSTD) method [2], [3]. The FDTD technique has been employed to study optical characteristics of biological cells [4]. The near-field electromagnetic wave interaction can be simulated using the FDTD algorithm, whereas the far-field scattered light intensity as a function of angle, the radar cross-section (RCS), can be determined via a near-to-far-field transformation [1], [5]. However, due to coherent interference (*speckle effects*), it is difficult to obtain general scattering characteristics of the random medium.

Defined as the sum of RCS of all angles, the total scattering cross-section (TSCS) is less vulnerable to speckle effects and is commonly used to characterize the optical properties of macroscopic random media [6], [7]. It is a better representation of the overall scattering characteristics than the RCS of a particular scattering angle. Other than summing up the RCS at all angles to obtain TSCS, the optical theorem enables determining the TSCS by the scattering light in the forward direction [8]. The optical theorem is also used in other research areas such as localized surface plasmon research [9] and RF antenna design [10]. In practical situations where the scattering amplitude is not known at all angles, the optical theorem can be very useful in determining the TSCS with *only* the scattering light in the forward scattering direction.

In this manuscript, we derive the practical relationship to employ the optical theorem in an FDTD simulation of light scattering problems. Furthermore, we analyze and compare the TSCS calculated based upon optical theorem with other methods.

Manuscript received June 28, 2009; revised November 05, 2009; accepted March 19, 2010. Date of publication June 14, 2010; date of current version September 03, 2010.

C.-H. Tsai is with the Graduate Institute of Photonics and Optoelectronics, National Taiwan University, Taipei 106, Taiwan.

S.-H. Chang is with the Institute of Electro-Optical Science and Engineering, National Cheng Kung University, Tainan 701, Taiwan.

S. H. Tseng is with the Department of Electrical Engineering, National Taiwan University, Taipei, Taiwan 106.

Color versions of one or more of the figures in this communication are available online at http://ieeexplore.ieee.org.

Digital Object Identifier 10.1109/TAP.2010.2052556

II. Derivation

The near-field light scattering interaction can be simulated using the FDTD technique; generally after a near-to-far-field transformation, the absolute value of the far-field scattering amplitude in terms of RCS is obtained. However, the optical theorem requires only the real part instead of the absolute value of the forward scattered light; thus, in order to calculate TSCS by means of the optical theorem in an FDTD simulation, it is necessary to modify the expressions of optical theorem, so that the parameters involved in the optical theorem can be directly obtained from the FDTD simulation.

We modify the optical theorem expression to match the parameters given in the FDTD simulation. The 2D TM_z mode optical theorem is given by [8]:

$$C_{ext,TM} = \frac{4}{k}\mathrm{Re}\{T_1(\theta = 0)\} \tag{1}$$

where k is the wavenumber corresponding to the wavelength. The scattering amplitude $T_1(\theta)$ is a function of scattering angle θ as defined in [8]. The phasor relationship of the incident electric field $\vec{E}_i = E_{zi}\hat{z}$ and the far-field scattered electric field $E_{zs}(\theta)\hat{z}$ is

$$E_{zs}(\theta)e^{-i\omega t} = e^{-i(3/4)\pi}\sqrt{\frac{2}{\pi kr}}e^{ikr}T_1(\theta)E_{zi}e^{-i\omega t}. \tag{2}$$

In the FDTD context, the complex-valued pattern function $F_{TM}(\varphi)$ describes the far-field scattered electric field *phasor* $\check{E}_{zs}(\varphi)$ as [1]

$$\check{E}_{zs}(\varphi)e^{i\omega t} = \frac{e^{-ikr}}{\sqrt{r}}F_{TM}(\varphi)e^{i\omega t}. \tag{3}$$

The scattering angle defined in [1] and [8], θ and φ, are related by $\theta = -\varphi$. $F_{TM}(\varphi)$ is a complex-valued pattern function as a function of scattering angle φ, defined as

$$F_{TM}(\varphi) = \frac{e^{i(\pi/4)}}{\sqrt{8\pi k}}\oint\begin{bmatrix}-\omega\mu_0\hat{\mathbf{z}}'\cdot\check{\mathbf{J}}_{\mathbf{eq}}(\mathbf{r}') \\ -k\hat{\mathbf{z}}'\times\check{\mathbf{M}}_{\mathbf{eq}}(\mathbf{r}')\cdot\hat{\mathbf{r}}\end{bmatrix}e^{ik\hat{\mathbf{r}}\cdot\mathbf{r}'}dC' \tag{4}$$

C' is a closed contour surrounding the scatterer, r and r' are position vectors, $\hat{r}$ is the unit vector of r, and $\hat{z}'$ is the unit vector in the z' direction [1]. The equivalent electric current $\check{\mathbf{J}}_{\mathbf{eq}}$ and equivalent magnetic current $\check{\mathbf{M}}_{\mathbf{eq}}$ are defined by

$$\begin{aligned}\check{\mathbf{J}}_{\mathbf{eq}}(\omega,\mathbf{r}') &= \hat{\mathbf{n}}\times\check{\mathbf{H}}_{\mathbf{s}}(\omega,\mathbf{r}')\\ \check{\mathbf{M}}_{\mathbf{eq}}(\omega,\mathbf{r}') &= -\,\hat{\mathbf{n}}\times\check{\mathbf{E}}_{\mathbf{s}}(\omega,\mathbf{r}').\end{aligned} \tag{5}$$

The complex *phasors* $\check{\mathbf{H}}_{\mathbf{s}}$, $\check{\mathbf{E}}_{\mathbf{s}}$ are obtained by Fourier transform of the FDTD calculated time-domain scattered electromagnetic fields. Notice that (2) and (3) both describe the far-field scattered electric field with slightly different terms involved: $e^{-i\omega t}$ in the optical theorem context [(2)], but $e^{+i\omega t}$ in the FDTD context [(3)]. By taking the complex conjugate of $\check{E}_{zs}(\varphi)$, (2) and (3) can be combined into

$$\begin{aligned}\check{E}^*_{zs}(\varphi=0)e^{-i\omega t} &= \frac{e^{ikr}}{\sqrt{r}}F^*_{TM}(\varphi=0)e^{-i\omega t}\\ &= E_{zs}(\theta=0)e^{-i\omega t}\\ &= e^{-i(3/4)\pi}\sqrt{\frac{2}{\pi kr}}T_1(\theta=0)E_{zi}e^{-i\omega t}.\end{aligned} \tag{6}$$

After re-arranging (6), the relationship of scattering amplitude $T_1(\theta)$ and the complex-valued pattern function $F_{TM}(\varphi)$ can be expressed as

$$\begin{aligned} T_1(\theta=0) &= \sqrt{\frac{\pi k}{2}} e^{-i(3/4)\pi} \frac{F_{TM}^*(\varphi=0)}{E_{zi}} \\ &= \sqrt{\frac{\pi k}{2}} e^{-i(3/4)\pi} \frac{F_{TM}^*(\varphi=0)}{\check{E}_i^*}. \end{aligned} \tag{7}$$

The term $e^{i\omega t}$ must be carefully accounted for to yield $E_{zi} = \check{E}_i^*.\check{E}_i$ is the initial incident electric field $E_i(t, \mathbf{r}=\mathbf{0})$ after Fourier transform. Lastly, by inserting $T_1(\theta=0)$ of (7) into (1), we arrive at

$$\begin{aligned} C_{ext,TM} &= \frac{4}{k} \mathrm{Re}\{T_1(\theta=0)\} \\ &= \sqrt{\frac{8\pi}{k}} \mathrm{Re}\left\{ e^{-i(3/4)\pi} \left[\frac{F_{TM}(\varphi=0)}{\check{E}_i(\mathbf{r}=0)} \right]^* \right\}. \end{aligned} \tag{8}$$

Similarly, an expression of the optical theorem for the $\mathrm{TE_z}$ mode can be derived

$$C_{ext,TE} = \sqrt{\frac{8\pi}{k}} \mathrm{Re}\left\{ e^{-i(3/4)\pi} \left[\frac{F_{TE}(\varphi=0)}{\check{H}_i(\mathbf{r}=0)} \right]^* \right\} \tag{9}$$

with the complex-valued pattern function $F_{TE}(\varphi)$ in (9) defined by [1]

$$F_{TE}(\varphi) = \frac{e^{i(\pi/4)}}{\sqrt{8\pi k}} \oint \begin{bmatrix} -\omega\varepsilon_0 \hat{\mathbf{z}}' \cdot \check{\mathbf{M}}_{\mathbf{eq}}(\mathbf{r}') \\ +k\hat{\mathbf{z}}' \times \check{\mathbf{J}}_{\mathbf{eq}}(\mathbf{r}') \cdot \hat{\mathbf{r}} \end{bmatrix} e^{ik\hat{\mathbf{r}}\cdot\mathbf{r}'} dC' \tag{10}$$

Notice that the optical theorem requires *only the real part* of the scattered field, therefore, the $RCS(\varphi=0)$ obtained from the FDTD simulation cannot be used directly in the optical theorem to calculate TSCS. *It is necessary to separate the real part and imaginary part of the scattered field in an FDTD simulation in order to employ the optical theorem to calculate the TSCS.*

III. METHOD

Here we present determining the TSCS of a *non-absorbing* dielectric cylinder via various methods and compare their accuracies. The accuracy of the calculated TSCS is determined by comparing with the analytical solution of Maxwell's equations—Mie theory [11]. Four methods are employed to calculate the TSCS: a) optical theorem, b) Sum of far-field RCS at all angles c) Near-field outgoing Poynting vector flux, and d) Definition of extinction cross-section (ECS). A brief description of each method is shown as follows:

A. Optical Theorem

The calculation of TSCS by means of the optical theorem in an FDTD simulation is described in Section II. The TSCS for $\mathrm{TM_z}$ mode incident light can be calculated via (8); for $\mathrm{TE_z}$ mode, incident light can be calculated via (9).

B. Sum of Far-Field RCS at All Angles

TSCS represents the "total" scattering effectiveness of the sample and can be calculated by the sum of RCS of all angles [8]. The near-to-far-field transformation of the FDTD simulation yields RCS at all angles which can be used to calculate TSCS by integrating all angles of RCS along a large cylindrical surface of radius r. For $r \to \infty$, the Poynting vector in the far-field becomes: $\mathbf{S_s} = |\mathbf{S_s}|\hat{r}$. With dl replaced by $rd\varphi$ and $d\varphi$ replaced by $\lim_{N\to\infty} 2\pi/N$, the TSCS (C_{sca}) can be calculated by

$$C_{sca} = \lim_{r\to\infty} \frac{1}{I_i} \oint \mathbf{S_s} \cdot \hat{r} dl = \lim_{N\to\infty} \sum_{n=1}^{N} RCS(\varphi_n) \frac{1}{N} \tag{11}$$

$\mathbf{S_s}$ is the time-averaged Poynting vector of the scattered field; I_i is the time-averaged Poynting vector of the incident field.

C. Near-Field Outgoing Poynting Vector Flux

Instead of calculating TSCS using far-field scattered light information, the TSCS can also be obtained using near-field Poynting vector flux

$$C_{sca} = \frac{1}{I_i} \oint \mathbf{S_s} \cdot d\vec{l} \tag{12}$$

$$\mathbf{S_s} = \frac{1}{2} \mathrm{Re}\left\{ \mathbf{E_s} \times \mathbf{H_s^*} \right\}. \tag{13}$$

The TSCS basically can be determined by integrating the scattered field along an arbitrary closed surface; for convenience, we integrate the scattered field along a rectangular-shaped closed surface of the FDTD simulation grid.

Definition of ECS

By definition, the ECS is the sum of the TSCS and the absorption cross-section: $C_{est} = C_{sca} + C_{abs}$, thus, for a non-absorbing scatterer $(C_{abs} = 0)$, the ECS (C_{ext}) is equal to the TSCS (C_{sca}). Therefore, the TSCS can also be obtained according to the definition of the ECS

$$C_{ext} = -\frac{1}{I_i} \oint \mathbf{S}_{ext} \cdot d\vec{l} \tag{14}$$

$$\mathbf{S_{ext}} = \frac{1}{2} \mathrm{Re}\left\{ \mathbf{E_i} \times \mathbf{H_s^*} + \mathbf{E_s} \times \mathbf{H_i^*} \right\}. \tag{15}$$

IV. SIMULATION RESULTS

In this manuscript, we simulate $\mathrm{TE_z}$ mode light scattering by a non-absorbing dielectric cylinder in 2-D. The excitation source is a temporal impulsive plane wave in the time domain. The radius of the dielectric cylinder is 5 μm, with a refractive index of $n = 1.2$. The FDTD simulation is performed with a grid resolution $\Delta s = 1/60\ \mu\mathrm{m}$, $1/80\ \mu\mathrm{m}$, $1/100\ \mu\mathrm{m}$, $1/120\ \mu\mathrm{m}$, $1/140\ \mu\mathrm{m}$, $1/160\ \mu\mathrm{m}$, $1/180\ \mu\mathrm{m}$, and $1/200\ \mu\mathrm{m}$, respectively. The observed frequency ranges from 100 THz to 750 THz, with an interval of 5 THz.

The TSCS as a function of frequency is compared with the Mie analytical solution as shown in Figs. 1 and 2. Fig. 1 corresponds to an FDTD simulation with a grid resolution of $\Delta s = 1/60\ \mu\mathrm{m}$, and Fig. 2 corresponds to a grid resolution of $\Delta s = 1/120\ \mu\mathrm{m}$. The x-axis represents the light frequency ranging from 100 THz to 750 THz, and the y-axis represents the TSCS $(\mu\mathrm{m})$.

Figs. 1 and 2 clearly show that the TSCS calculated via each method is accurate compared to Mie theory. With a finer FDTD grid resolution, the TSCS calculated in the FDTD simulation asymptotically matches Mie theory. This is expected since the FDTD simulation is a rigorous simulation technique based on a 2nd order numerical solutions

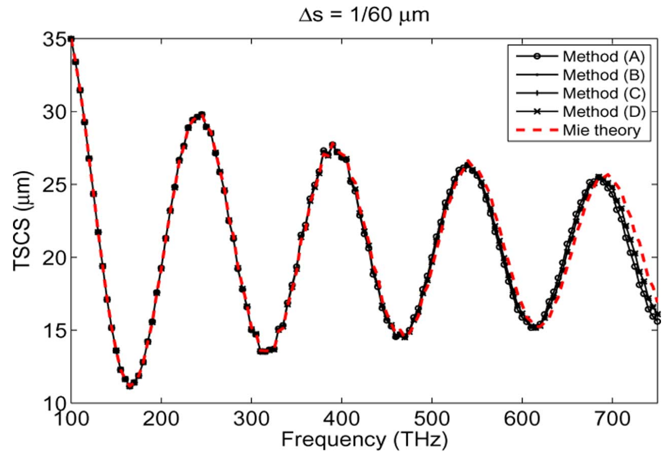

Fig. 1. Compare TSCS calculated via various methods in an FDTD simulation with grid resolution $\Delta s = 1/60\ \mu\mathrm{m}$. Methods (A): optical theorem, (B): Sum of far-field RCS at all angles, (C): Near-field outgoing Poynting vector flux, and (D): Definition of ECS.

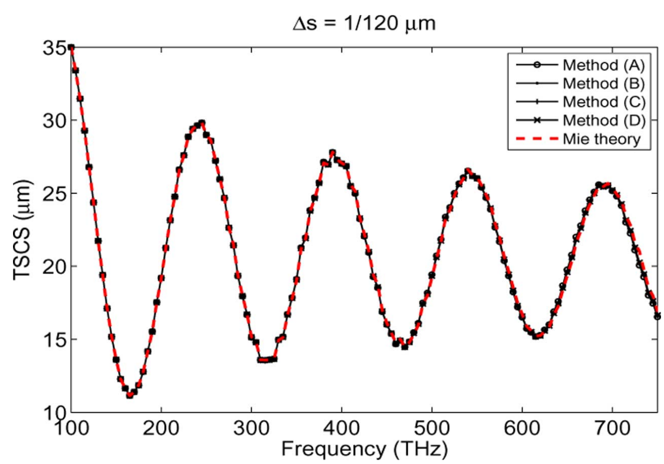

Fig. 2. Compare TSCS calculated via various methods in an FDTD simulation with grid resolution $\Delta s = 1/120\ \mu\mathrm{m}$.

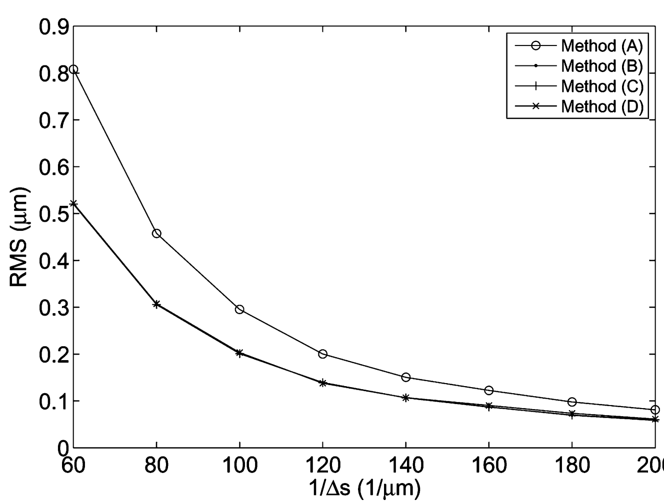

Fig. 3. Compare RMS error of the TSCS calculation in an FDTD simulation.

of Maxwell's equations. The RMS error as a function of $1/\Delta s(1/\mu\mathrm{m})$ is depicted in Fig. 3.

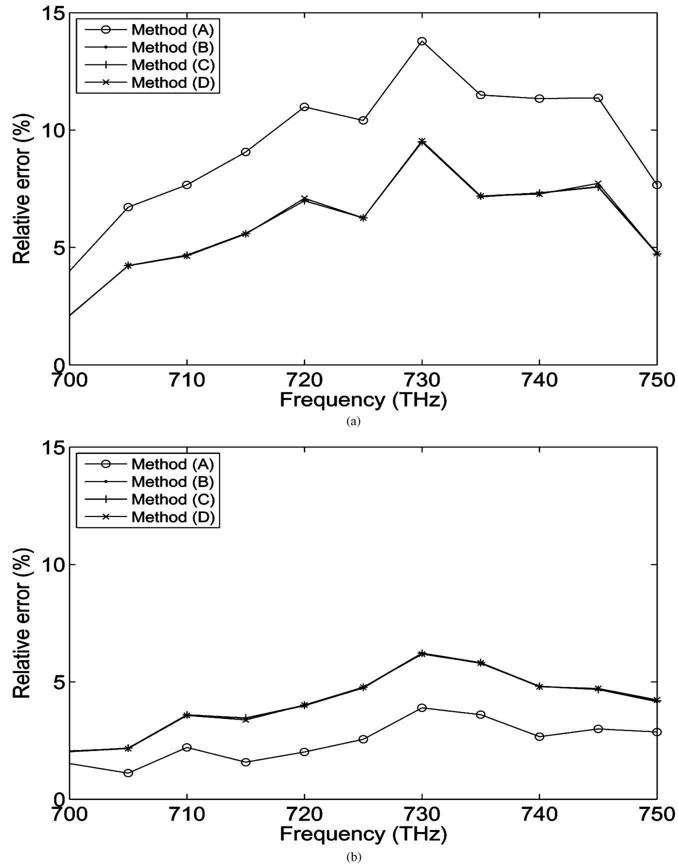

Fig. 4. Error of TSCS calculation via various methods compared with Mie theory. The FDTD simulation is performed with an FDTD grid resolution of $\Delta s = 1/60\ \mu\mathrm{m}$. (a) The error of TSCS calculated via optical theorem is larger than others; (b) After compensating for the numerical dispersion of a frequency of 750 THz at 0 degree, the accuracy of optical theorem calculated TSCS exceeds others.

V. Discussions

The accuracy of the TSCS calculated by each method is compared and shown in Fig. 3. The convergence analysis of Fig. 3 clearly shows that TSCS can be calculated by summing far-field RCS at all angles [method (B)], near-field information [method (C) and (D)], or simply with only the far-field forward scattered light [method (A)]. Analysis of the simulation results show that each of the four TSCS calculation methods is of 2nd order accurate and converges to the analytical solutions of Maxwell's equations.

Notice that in Fig. 3, the TSCS calculated by optical theorem exhibits larger error than the others. This can be accounted for by the anisotropy of the FDTD simulation grid. The conventional FDTD algorithm is based on a Cartesian grid, thus, the speed of light propagation in oblique directions and in parallel or perpendicular directions differ. The anisotropy is most severe in the forward (0 degree) scattering direction. As a result, the TSCS calculated via optical theorem which utilizes only the forward scattered light resulting in largest error, whereas other methods involve integration of all scattering angle, resulting in relatively lesser error, as shown in Fig. 4(a).

Method (A) is calculated based upon only the forward scattered light, thus, the numerical inaccuracy due to the FDTD grid anisotropy can be effectively suppressed [1]. By compensating for the numerical speed of light in the FDTD simulation for scattering angle of 0 degree (forward direction) at a particular incident frequency (750 THz), the error due to grid anisotropy can be significantly suppressed. The resulting accuracy of the TSCS calculated via optical theorem then exceeds the accuracy of other three methods, as shown in Fig. 4(b).

The proposed method (A) is also much more efficient than method (B) in calculating the TSCS. Method (B) requires a fine RCS function to achieve high enough accuracy, for a 2-D problem, typically requires RCS with an angular resolution of $\Delta\theta = 0.5^\circ$ (720 RCS values), as supposed to method (A) which only requires *one* single RCS value to calculate TSCS, the run-time of method (A) (optical theorem) is typically ~ 720 times faster than method (B). For a 3-D problem, method (A) becomes even more computationally efficient than method (B): TSCS can be calculated much faster with a factor of $\sim 2.6 \times 10^5$.

VI. Conclusions

In this communication, we report derivation and implementation details to employ the optical theorem for an FDTD light scattering simulation and show that the proposed method can be very pragmatic and accurate for determining the TSCS. The TSCS is conventionally calculated by summing up RCS of all scattering angles (Method B). However, to achieve high enough accuracy, the sum of a high resolution RCS as a function of scattering angle is necessary, resulting in more calculation and longer processing time. Instead of summing RCS at every scattering angle, we have derived and shown (Method A) that, based upon the optical theorem, the TSCS can be accurately determined with just *one* RCS value—RCS in the forward scattering direction (0 degree). (For 3D problems, obtaining the TSCS with only one RCS value becomes dramatically more efficient.) For practical calculation of TSCS where the scattering amplitude is not available for all scattering angles, the TSCS calculation by means of the optical theorem can be very useful; in addition, the numerical error due to anisotropy of the FDTD simulation can be reduced. The proposed method is based on the optical theorem and is generally applicable to light scattering problems of an isolated scatterer. More importantly, the proposed method is also applicable to general electromagnetic scattering problems including microwave-frequency regime.

References

[1] A. Taflove and S. C. Hagness*, Computational Electrodynamics: The Finite-Difference Time-Domain Method*. Boston: Artech House, 2005.

[2] Q. H. Liu, "The PSTD algorithm: A time-domain method requiring only two cells per wavelength," *Microw. Opt. Technol. Lett.*, vol. 15, pp. 158–165, Jun. 1997.

[3] Q. H. Liu, "Large-scale simulations of electromagnetic and acoustic measurements using the pseudospectral time-domain (PSTD) algorithm," *IEEE Trans. Geosci. Remote Sensing*, vol. 37, pp. 917–926, Mar. 1999.

[4] R. Drezek, A. Dunn, and R. Richards-Kortum, "A pulsed finite-difference time-domain (FDTD) method for calculating light scattering from biological cells over broad wavelength ranges," *Opt. Express*, vol. 6, pp. 147–157, Mar. 2000.

[5] P. W. Zhai, Y. K. Lee, G. W. Kattawar, and P. Yang, "Implementing the near- to far-field transformation in the finite-difference time-domain method," *Appl. Opt.*, vol. 43, pp. 3738–3746, 2004.

[6] S. H. Tseng, J. H. Greene, A. Taflove, D. Maitland, V. Backman, and J. Walsh, "Exact solution of Maxwell's equations for optical interactions with a macroscopic random medium," *Opt. Lett.*, vol. 29, pp. 1393–1395, Jun. 2004.

[7] S. H. Tseng, J. H. Greene, A. Taflove, D. Maitland, V. Backman, and J. T. Walsh, "Exact solution of Maxwell's equations for optical interactions with a macroscopic random medium: Addendum," *Opt. Lett.*, vol. 30, pp. 56–57, Jan. 2005.

[8] G. F. A. Bohren and D. R. Huffman*, Absorption and Scattering of Light by Small Particles*. New York: Wiley, 1983.

[9] T. Pakizeh, M. S. Abrishamian, N. Granpayeh, A. Dmitriev, and M. Kall, "Magnetic-field enhancement in gold nanosandwiches," *Opt. Express*, vol. 14, pp. 8240–8246, 2006.

[10] V. Villamizar and O. Rojas, "Time-dependent numerical method with boundary-conforming curvilinear coordinates applied to wave interactions with prototypical antennas," *J. Comput. Phys.*, vol. 177, pp. 1–36, 2002.

[11] G. Mie, "Articles on the optical characteristics of turbid tubes, especially colloidal metal solutions," *Annalen Der Physik*, vol. 25, pp. 377–445, 1908.

Optimization of Reduced-Size Smooth-Walled Conical Horns Using BoR-FDTD and Genetic Algorithm

Anthony Rolland, Mauro Ettorre, M'Hamed Drissi, Laurent Le Coq, and Ronan Sauleau

***Abstract*—An accurate optimization tool has been developed to design arbitrarily-shaped axis-symmetrical devices. It is based on the combination between a genetic algorithm (GA) and a finite-difference time-domain (FDTD) solver formulated in a cylindrical coordinate system. For validation purposes, this tool is applied to design several smooth-walled compact conical horns with a large flare angle (90°) in the 60-GHz band. The unavoidable phase distortions appearing in the horn aperture are compensated by loading the horn mouth with thin shaped dielectric lenses made in Rexolite. Based on these test cases, several synthesis strategies are discussed and compared in order to select the best antenna prototype among those synthesized. A scaled version of this prototype has been fabricated to operate around 29.5 GHz. The numerical and experimental results are in excellent agreement. Horn size reduction rates up to 80% have been reached.**

***Index Terms*—BoR-FDTD, dielectric lens, genetic algorithm, millimeter waves, optimization, smooth-walled conical horns.**

I. Introduction

Three-dimensional (3-D) bodies of revolution (BoR) [1], [2] are very attractive since they are simple to fabricate and cover a wide family of microwave and millimeter-wave devices like UWB antennas [3], conical and corrugated horns [4]–[6], or axis-symmetrical reflectors [7], [8] and lenses [9], [10]. By virtue of circular symmetry, their electromagnetic characteristics can be determined rigorously by reducing the original 3-D problem to a two-dimensional and half one. Consequently the computation time needed to completely perform one full-wave analysis of BoR devices becomes short enough to envisage combining the corresponding analysis kernels with iterative optimization algorithms. In other words this paves the way for the automatic electromagnetic synthesis of BoR.

In this frame, if we only consider BoR, various numerical formulations (finite elements [3], mode matching techniques [4], [5] and high-frequency methods [9], [11], [12]) have been coupled recently to optimization routines based on gradient methods [5], [13], [14], simulated annealing [3], particle swarm optimization [4] and GAs [5], [9].

Manuscript received July 02, 2009; revised February 23, 2010; accepted February 24, 2010. Date of publication June 14, 2010; date of current version September 03, 2010. This work was supported in part by the "Université Européenne de Bretagne" (UEB), France under the "International Chair" program and the OPTIMISE project, and in part by the Conseil Régional de Bretagne (CREATE/CONFOCAL project).

The authors are with the Institute of Electronics and Telecommunications of Rennes (IETR), UMR CNRS 6164, University of Rennes 1 and INSA de Rennes, Rennes, France (e-mail: ronan.sauleau@univ-rennes1.fr).

Digital Object Identifier 10.1109/TAP.2010.2052557